Journal of Alzheimer's Disease 47 (2015) 117–127
DOI 10.3233/JAD-150049
IOS Press

Non-Linear Association between Cerebral Amyloid Deposition and White Matter Microstructure in Cognitively Healthy Older Adults

Dominik Wolf*, Florian U. Fischer, Armin Scheurich, Andreas Fellgiebel and for the Alzheimer's Disease Neuroimaging Initiative[1]
Department of Psychiatry and Psychotherapy, University Medical Center Mainz, Mainz, Germany

Handling Associate Editor: Babak Ardekani

Accepted 8 April 2015

Abstract. Cerebral amyloid-β accumulation and changes in white matter (WM) microstructure are imaging characteristics in clinical Alzheimer's disease and have also been reported in cognitively healthy older adults. However, the relationship between amyloid deposition and WM microstructure is not well understood. Here, we investigated the impact of quantitative cerebral amyloid load on WM microstructure in a group of cognitively healthy older adults. AV45-positron emission tomography and diffusion tensor imaging (DTI) scans of forty-four participants (age-range: 60 to 89 years) from the Alzheimer's Disease Neuroimaging Initiative were analyzed. Fractional anisotropy (FA), mean diffusivity (MD), radial diffusivity (DR), and axial diffusivity (DA) were calculated to characterize WM microstructure. Regression analyses demonstrated non-linear (quadratic) relationships between amyloid deposition and FA, MD, as well as RD in widespread WM regions. At low amyloid burden, higher deposition was associated with increased FA as well as decreased MD and DR. At higher amyloid burden, higher deposition was associated with decreased FA as well as increased MD and DR. Additional regression analyses demonstrated an interaction effect between amyloid load and global WM FA, MD, DR, and DA on cognition, suggesting that cognition is only affected when amyloid is increasing and WM integrity is decreasing. Thus, increases in FA and decreases in MD and RD with increasing amyloid load at low levels of amyloid burden may indicate compensatory processes that preserve cognitive functioning. Potential mechanisms underlying the observed non-linear association between amyloid deposition and DTI metrics of WM microstructure are discussed.

Keywords: ADNI, cerebral amyloid deposition, cognitively healthy older adults, quadratic polynomial regression analyses, tract-based spatial statistics, white matter microstructure

[1]Data used in preparation of this article were obtained from the Alzheimer's Disease Neuroimaging Initiative (ADNI) database (http://adni.loni.usc.edu). As such, the investigators within the ADNI contributed to the design and implementation of ADNI and/or provided data but did not participate in analysis or writing of this report. A complete listing of ADNI investigators can be found at: http://adni.loni.usc.edu/wp-content/uploads/how_to_apply/ADNI_Acknowledgement_List.pdf.

*Correspondance to: Dr. Dominik Wolf, Department of Psychiatry and Psychotherapy, University Medical Center Mainz, Untere Zahlbacher Str. 8, 55131 Mainz, Germany. Tel.: +49 6131 172488; Fax: +49 6131 176690; E-mail: dominik.wolf@unimedizin-mainz.de.

ISSN 1387-2877/15/$35.00

INTRODUCTION

Cerebral amyloid-β (Aβ) plaques are hallmark neuropathological markers of Alzheimer's disease (AD) [1]. Significant amyloid accumulation has also been observed in 10–30% of cognitively healthy older adults, suggesting that the presence of brain amyloidosis is not sufficient to produce cognitive symptoms [2, 3]. Besides cerebral amyloid accumulation, both AD patients as well as cognitively healthy older adults commonly show substantial changes in white matter (WM) microstructure. These changes have frequently been linked to cognitive deficits [4, 5]. The association between cerebral amyloid deposition and WM microstructure is not well understood. However, a more thorough understanding of this relationship is necessary to gain deeper insights into mechanisms leading to cognitive decline and to improve prediction of future AD.

A frequently applied method to characterize WM microstructure *in vivo* is diffusion tensor imaging (DTI), which measures the random thermal diffusion of water molecules in biological tissues and thereby permits an indirect reconstruction of the microstructural organization of cerebral WM [6]. The most commonly used DTI metrics are fractional anisotropy (FA), mean diffusivity (MD), radial diffusivity (DR), and axial diffusivity (DA). FA is a scalar measure of the directional coherence of water diffusion and reflects the organization of neuronal elements particularly within myelinated fiber bundles [7]. MD is a measure of the overall diffusion and indicates microscopic barriers or obstacles in both gray and white matter [7]. The DTI metrics DR and DA characterize microscopic water diffusion parallel to (DA) or perpendicular to (DR) the main diffusion direction [8]. DTI metrics have been proposed to be surrogate markers of microstructural WM integrity [9].

Previous DTI studies investigating the association between cerebral amyloid deposition and WM microstructure differ largely in terms of investigated brain regions, DTI metrics, and diagnostic status. Moreover, studies have been performed in transgenic mouse models as well as in human subjects. Early studies investigating transgenic mice overexpressing mutant amyloid-β precurser protein (AβPP) reported positive correlations between amyloid deposition and WM abnormalities in widespread WM tracts, including cerebral peduncle, corpus callosum, external capsule, and fornix [10, 11]. These results suggest greater axonal and myelin degeneration with increasing amyloid deposition. In line with these results, a more recent study found lower FA in the corpus callosum and fimbria in AβPP mice compared to wild-type controls [12]. However, other studies have been published that report higher FA in several white matter tracts, including corpus callosum, external capsule, cingulum, septum, internal capsule, fimbria, and optic tract in AβPP mice compared to wild-type controls [13, 14].

Inconsistent results have also been reported in human subjects. A study by Chao et al. found lower FA in fornix and corpus callosum in participants with high amyloid load compared to participants with low amyloid load in subjects spanning the spectrum of cognitively normal to mild cognitive impairment (MCI) [15]. In contrast, in a group of cognitively healthy elderly, Racine et al. demonstrated higher FA and lower MD in participants with high amyloid burden compared to participants with lower amyloid burden in the cingulum and lateral fornix [16]. Another study by Ryan et al. compared DTI measures of cerebral WM of healthy controls to those of presymptomatic and symptomatic participants who harbored genetic mutations for early onset AD. Presymptomatic subjects showed lower MD in the cingulum compared to healthy controls. In contrast, symptomatic subjects showed higher MD, DR, and DA and lower FA in widespread WM tracts (including corpus callosum, fornix, cingulum) [17].

Taken together, heterogeneous results regarding the association between amyloid deposition and WM microstructure (as measured by DTI) have been reported in both AβPP transgenic mice as well as in human subjects. Contradictory associations have even been observed in the same WM tracts (e.g., corpus callosum, fimbria). The heterogeneity in results indicates a complex relationship between amyloid deposition and WM microstructure. Of note, increases in FA and decreases in MD with increasing amyloid load in humans have only been observed in cognitively healthy elderly, while MCI and AD patients normally show an inverse relationship. Thus, the association between amyloid and WM microstructure may be modulated by the level of amyloid burden. In this exploratory study, we aimed at testing this hypothesis in a group of cognitively healthy older adults. Quadratic polynomial regression analyses were applied to characterize the relationship between cerebral amyloid deposition and global WM microstructure, as quantified by the mean FA, MD, DR, and DA within a WM skeleton. Moreover, voxel-wise quadratic regression analyses were performed to investigate the association between cerebral amyloid load and regional WM microstructure.

MATERIALS AND METHODS

The data underlying this study were obtained from the Alzheimer's Disease Neuroimaging Initiative (ADNI) database (http://adni.loni.usc.edu). ADNI is an ongoing project that was launched in 2003 with the primary goal of investigating neuroimaging, neuropsychiatric, and other biological measurements with regard to their utility as *in vivo* markers of AD pathogenesis. A more detailed and up-to-date description of ADNI can be found at http://www.adni-info.org.

Study group

The data of 44 cognitively normal older adults were analyzed in this study. Participants were selected according to the following procedure (see Fig. 1): At first, cognitively normal participants who received T1-weighted imaging, DTI, and florbetapir (AV45) positron emission tomography (PET) were selected from the ADNI database (ADNI/ADNI-GO/ADNI2, downloaded in 05/2014). In a next step, outliers, participants with extensive WM pathology, and participants with corrupted imaging scans (DTI or AV45 PET) were excluded, yielding in 44 participants who were included in this study. Outliers were identified using the Grubb's test ($p < 0.05$) [18]. Extensive WM pathology was defined as a visual Fazekas scale rating of 3 based on the T1-weighted images [19]. Detailed information regarding the classification as cognitively normal can be found at the ADNI website (http://adni.loni.usc.edu/methods).

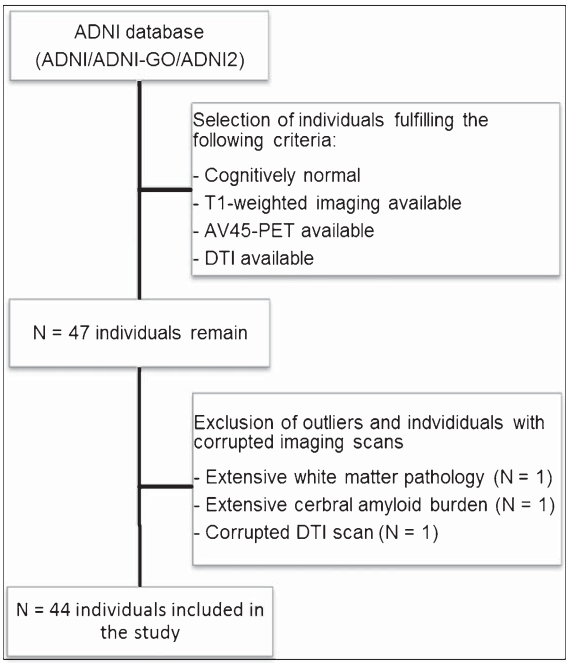

Fig. 1. Flow chart of the selection procedure of the study participants. ADNI, Alzheimer's Disease Neuroimaging Initiative; AV45-PET, Florbetapir positron emission tomography; DTI, diffusion tensor imaging.

Imaging data acquisition

DTI and T1-weighted data were acquired on multiple 3T MRI scanners (General Electric Healthcare) using scanner specific protocols. DTI acquisition was based in the following acquisition parameters: voxel size = $1.37^2 \times 2.70$ mm^3, 41 diffusion gradients and a b-value of 1000 s/mm^2.

AV45 PET imaging data were acquired on multiple types of scanners with varying resolution and platform-specific acquisition protocols. To increase data uniformity, original PET acquisitions in ADNI undergo a standardized preprocessing procedure.

More detailed information on the imaging protocols and specific preprocessing steps for PET acquisitions can be found at the ADNI website (http://adni.loni.usc.edu/methods).

DTI and T1-weighted data processing

DTI data were processed as described previously [20]. Briefly, processing of the data included the following steps: (a) motion and eddy current correction using FSL 5.0 (FMRIB Analysis Group, Oxford, UK, http://www.fmrib.ox.ac.uk/fsl) and adjustment of gradients, (b) removal of skull and non-brain tissue using Brain Extraction Tool [21], (c) fitting of diffusion tensors to the data and calculation of FA, MD, DR, and DA maps using CAMINO (http://cmic.cs.ucl.ac.uk/camino), based on the eigenvalues of the diffusion tensors [22]. Thereafter, Tract-Based Spatial Statistics (TBSS, [23]) was applied, including the following steps: (a) non-linear registration to the FMRIB58_FA template of all subjects' FA data using FMRIB's non-linear image registration tool [24], (b) creation and thinning of a mean FA image with a threshold 0.2 to obtain a mean FA skeleton that represented the centers of white matter trajectories, and (iii) projections of each subjects' aligned FA data onto the skeleton. To achieve skeletonized MD, DR, and DA data, the non-linear warps and skeleton projection vectors of the FA images were applied to the MD, DR, and DA data. Finally, mean FA, MD, DR, and DA values of the WM skeleton

were calculated for each individual, which represent different measures of global WM microstructure.

In order to calculate a continuous measure of WM hypointensity (WMH) volume, T1-weighted data were automatically segmented using Freesurfer (http://surfer.nmr.mgh.harvard.edu).

AV45-PET and T1-weighted data processing

Individual AV45-PET standardized uptake value ratios (SUVRs) were calculated by ADNI PET core laboratories and are available at the ADNI website (http://adni.loni.usc.edu/methods/pet-analysis). Briefly, cerebral AV45 uptake was quantified by the mean uptake within a composite mask including frontal, angular/posterior cingulate, lateral parietal, and lateral temporal regions, divided by the mean uptake within the cerebellum.

Statistics

In a first step, we analyzed the relationship between measures of global WM microstructure and cerebral amyloid load. Analyses were performed using the Statistics Software Package for Social Sciences (SPSS, v.21). Thereafter, we applied voxel-wise regression analyses using TBSS in order to examine the association between cerebral amyloid load and regional WM microstructure.

Analyses of global WM microstructure

Linear and quadratic polynomial regression analyses were applied and compared. Global DTI metrics (FA, MD, DR, and DA) were set as dependent variables. Cerebral AV45 uptake was set as independent variable. The quadratic model was built by squaring the AV45 uptake and adding this quadratic term to the linear model. Regression analyses were controlled for nuisance variables that were determined by testing the effect of potential confounding variables (i.e., age, education, gender, WMH, APOE4 genotype) on global DTI metrics using simple linear regression analyses (simple *t*-tests in case of APOE4 genotype). Variables that were significantly associated with at least one index of global WM microstructure were included as nuisance variable in all regression analyses. The variables of all regression analyses were mean-centered in order to reduce collinearity among predictors (the squared AV45 term was calculated from the mean-centered AV45 uptake). Residuals of all regression models were tested for deviance from normal distribution using the Kolmogorov-Smirnov test. Statistical significance was set at $p < 0.05$. To minimize type 1 errors due to multiple testing, a Bonferroni correction was used for independent testing. Since DTI metrics are not independent of each other, the *p*-value was adjusted for the number of different independent types of regression analyses that were applied ($n = 2$), resulting in an adjusted *p*-value of $p < 0.025$. The model fits of the linear and quadratic models were compared using the Akaike Information Criterion (AIC).

Voxel-wise analyses of WM microstructure

In order to explore the spatial distribution of potential quadratic associations between cerebral AV45 uptake and WM microstructure, voxel-wise quadratic polynomial regression analyses were applied using TBSS. DTI metrics were set as dependent variables. Cerebral AV45 uptake and its squared term were set as independent variables. Covariates of no interest were defined as described in the previous paragraph. Regression analyses were performed using the randomize tool, which tested a *t*-value at each voxel against a null distribution that was obtained from 5000 random permutations. Statistical significance was set at $p < 0.05$ corrected for multiple comparisons using threshold free cluster enhancement.

RESULTS

Demographic and descriptive characteristics of the study group are displayed in Table 1. Prior to the application of the main regression analyses, the influence of potential confounding variables (i.e., age, education, gender, WMH, ApoE4-genptype) on WM microstructure was tested. Simple regression analyses (simple *t*-test in case of ApoE4-genotype) demonstrated significant associations between age as well as WMH and at least one index of global WM microstructure. Gender, education, and ApoE4-genotype were not related to global FA, MD, DR, or DA. Accordingly, age and WMH were included as covariates of no interest in all linear and quadratic polynomial regression analyses.

Analyses of global WM microstructure

Results of the multiple linear and quadratic polynomial regression analyses of the relationship between cerebral AV45 uptake and global WM microstructure are displayed in Table 2. Simple scatterplots of these relationships are shown in Fig. 2. Comparisons of the model fits between the linear and the quadratic models

Table 1
Demographic and descriptive characteristics of the study group

Demographic characteristics	
n	44
Age (range)	73.01 ± 6.20 (60–89)
Gender	
Male	23
Female	21
Education years	16.30 ± 2.66
Descriptive characteristics	
WMH volume (cm^3)	3.36 ± 2.07
Cerebral AV45 SUVR uptake	1.06 ± 0.11
ApoE4	
Positive	13 (100% heterozygotes)
Negative	31
Global FA	0.45 ± 0.02
Global MD	0.74 ± 0.04
Global DR	0.54 ± 0.04
Global DA	1.15 ± 0.04

WMH, white matter hypointensities; Cerebral AV45 SUVR, cerebral Florbetapir standardized uptake value ratios; ApoE4, Apolipoprotein E type 4; Global FA, averaged fractional anisotropy of a tract-based spatial statistics (TBSS) skeleton; Global MD, averaged mean diffusivity of a TBSS skeleton; Global DR, averaged radial diffusivity of a TBSS skeleton; Global DA, averaged axial diffusivity of a TBSS skeleton.

(AIC) are given in Table 3. The linear regression models did not show an association between cerebral AV45 uptake and global FA, MD, RD, or DA. In contrast, the quadratic polynomial regression models demonstrated significant associations between the quadratic term of AV45 uptake and global FA ($p = 0.005$, inverted u-shaped association), global MD ($p = 0.021$, u-shaped association), as well as global DR ($p = 0.009$, u-shaped association). The association between the quadratic term of AV45 uptake and global DA was not significant ($p = 0.130$). The quadratic regression models showed better model fits than the linear models for global FA, MD, and DR as tested by the AIC (Akaike weights: FA = 23.66, MD = 5.73, DR = 13.68). For global DA, the model fit of the quadratic model was only slightly better than the model fit of the linear model (Akaike weight: DA = 1.03) (see Table 2).

Voxel-wise analyses of WM microstructure

Voxel-based mapping of the quadratic effects of AV45 uptake on DTI metrics using TBSS is shown in Fig. 3. In accordance with previous results, analyses demonstrated significant quadratic associations between cerebral AV45 uptake and FA as well as DR values (FA: inverted u-shaped association; DR: u-shaped association). These associations were widely distributed throughout large parts of the skeleton (including corpus callosum, fornix, corona radiata, internal/external capsule, and cingulum), instead of being locally pronounced. For MD, quadratic effects did not survive correction for multiple comparisons. At $p < 0.025$, uncorrected for multiple comparisons, significant quadratic associations between AV45 uptake and MD have been found in the corpus callosum, corona radiata, and cingulum (data not shown). For DA, no quadratic association with cerebral AV45 uptake was observed (see Fig. 3). Additional linear voxel-wise regression analyses did not show any associations between cerebral AV45 uptake and WM FA, MD, DR, or DA (data not shown).

Supplementary analyses

Additional multiple linear regression analyses were applied to investigate the association between cognitive performance and cerebral AV45 uptake, WM microstructure, as well as their interaction. Cognitive scores were set as dependent variables (ADNI composite scores of executive and memory function [25, 26]). Cerebral AV45 uptake, global DTI metrics, as well

Table 2
Results of linear and quadratic polynomial regression analyses

	Linear model[a]							Quadratic model[b]								
	AV45		Age		WMH			$AV45^2$		AV45		Age		WMH		
	beta	*p*	beta	*p*	beta	*p*	R^2	beta	*p*	beta	*p*	beta	*p*	beta	*p*	R^2
Global FA	−0.147	0.283	−0.246	0.112	−0.357	**0.023**	0.287	−0.482	**0.005**	0.151	0.351	−0.098	0.510	−0.429	**0.004**	0.410
Global MD	−0.081	0.553	0.343	0.031*	0.240	0.124	0.265	0.408	**0.021**	−0.333	0.052	0.218	0.165	0.302	0.046*	0.359
Global DR	−0.050	0.719	0.325	0.040*	0.263	0.094	0.260	0.460	**0.009**	−0.333	0.048*	0.184	0.231	0.332	0.027*	0.380
Global DA	−0.143	0.302	0.360	0.025*	0.179	0.250	0.254	0.276	0.130	−0.313	0.079	0.275	0.095	0.221	0.158	0.297

Global FA, averaged fractional anisotropy of a tract-based spatial statistics (TBSS) skeleton; Global MD, averaged mean diffusivity of a TBSS skeleton; Global DR, averaged radial diffusivity of a TBSS skeleton; Global DA, averaged axial diffusivity of a TBSS skeleton; AV45, cerebral amyloid load; $AV45^2$, squared term of cerebral amyloid load; WMH, white matter hypointensities; beta, standardized regression coefficient; R^2, percentage of explained variance of regression models/model fit; in bold: $p < 0.025$ (Bonferroni corrected *p*-value; *p*-value was adjusted for the number of independent regression types that were applied), *tendency to significance: $p < 0.05$ (uncorrected). [a]linear models: depend variables = global DTI metrics; independent variables = AV45, WMH, age. [b]quadratic models: depend variables = global DTI metrics; independent variables = $AV45^2$, AV45, WMH, age.

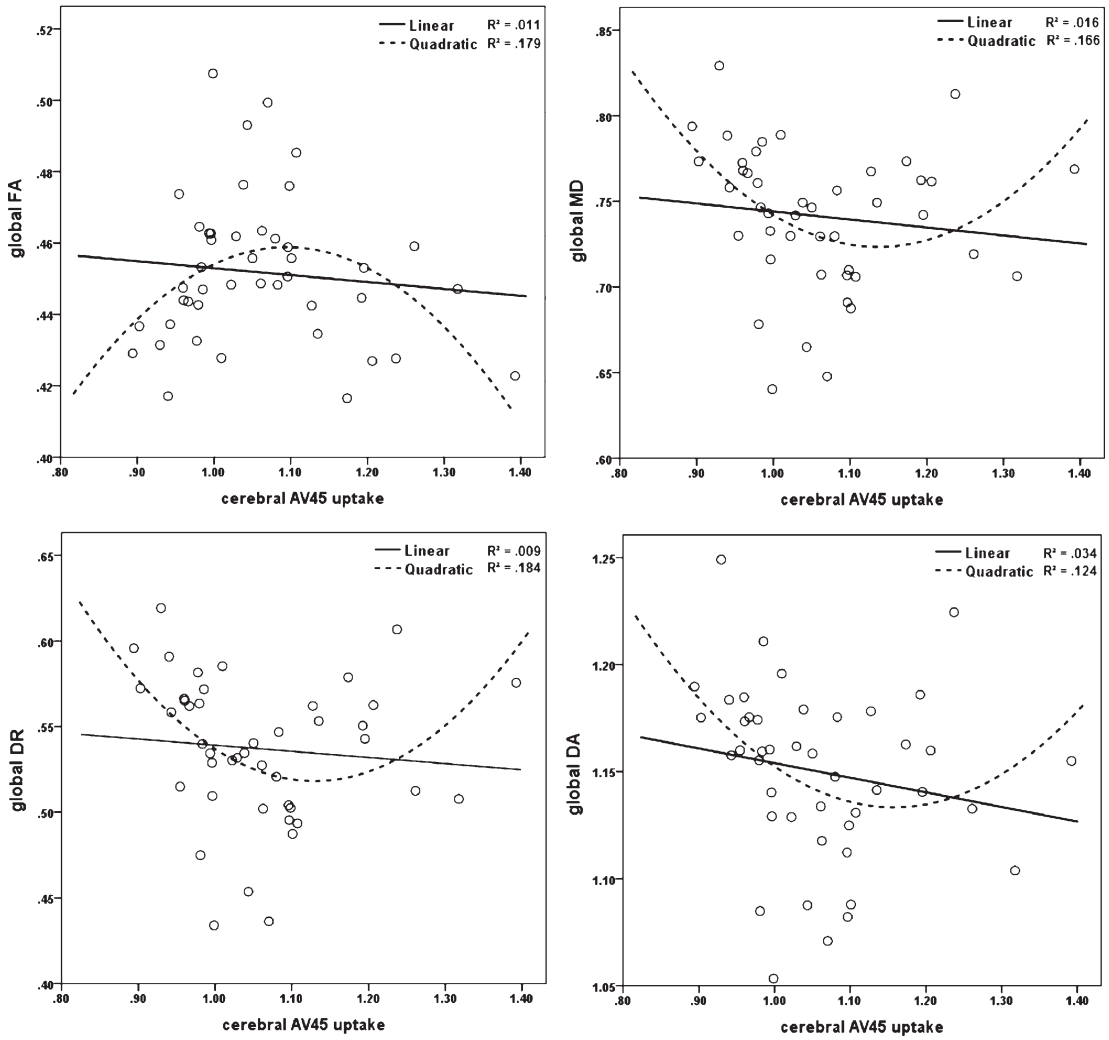

Fig. 2. Scatterplots of the relationship between cerebral amyloid load and DTI metrics of global WM microstructure; Global FA, averaged fractional anisotropy of a tract-based spatial statistics (TBSS) skeleton; Global MD, averaged mean diffusivity of a TBSS skeleton; Global DR, averaged radial diffusivity of a TBSS skeleton; Global DA, averaged axial diffusivity of a TBSS skeleton; Av45 uptake, cerebral Florbetapir standardized uptake value ratios; dashed line, simple quadratic model; continuous line, simple linear model; R^2, percentage of explained variance/model fit.

as their interaction were set as covariates of interest. In line with the previously described methodological procedure, covariates of no interest were determined by testing the effect of potential confounding variables (age, education, gender, WMH, ApoE-genotype) on the cognitive scores using simple linear regression analyses. Only age and WMH were associated with at least one of the investigated cognitive scores and thus included as covariates of no interest in all regression analyses. At a Bonferroni corrected threshold of $p < 0.025$ (corrected for the number of independent cognitive domains: $n = 2$), analyses demonstrated significant associations between executive functions and all interactions terms (AV45 × global FA: $p < 0.005$; AV45 × global MD: $p < 0.003$; AV45 X global DR: $p < 0.002$; AV45 × global DA: $p < 0.006$). No significant associations between memory functions and any of the interaction terms have been observed. Moreover, no main effects of cerebral AV45 uptake and global WM microstructure on cognitive scores have been found.

DISCUSSION

In this exploratory study, we aimed at testing if the association between cerebral amyloid deposition and

Table 3
Comparison of model fits between multiple linear and quadratic regression models

	AIC linear model[a]	AIC quadratic model[b]	Δ	*w*
Global FA	−347.70	−354.03	6.33	23.66[c]
Global MD	−286.31	−289.79	3.48	5.72[d]
Global DR	−283.16	−288.39	5.23	13.67[e]
Global DA	−286.48	−286.54	0.06	1.03[f]

Global FA, averaged fractional anisotropy of a tract-based spatial statistics (TBSS) skeleton; Global MD, averaged mean diffusivity of a TBSS skeleton; Global DR, averaged radial diffusivity of a TBSS skeleton; Global DA, averaged axial diffusivity of a TBSS skeleton; AIC, Akaike Information Criterion; Δ = difference in AIC between linear and quadratic model; *w*: Akaike weights. [a]linear models: depend variables = global DTI metrics; independent variables = cerebral amyloid load, white matter hypointensities, age. [b]quadratic models: depend variables = global DTI metrics; independent variables = cerebral amyloid load, squared term of cerebral amyloid load, white matter hypointensities, age. [c]the quadratic model is 24 times more likely to be correct than the linear model. [d]the quadratic model is 6 times more likely to be correct than the linear model. [e]the quadratic model is 14 times more likely to be correct than the linear model. [f]the quadratic model is 1 time more likely to be correct than the linear model.

WM microstructure is modulated by the level of amyloid burden in a group of cognitively healthy older adults. Importantly, regression analyses demonstrated a non-linear (quadratic) relationship between amyloid deposition and DTI metrics of WM microstructure. At low amyloid burden, higher amyloid deposition was associated with increased FA and decreased DR and MD. At higher amyloid burden, higher amyloid deposition was associated with decreased FA and increased DR and MD. These results might explain and link the heterogeneous and apparently contradictory findings of previous studies.

Non-linear association between cerebral amyloid deposition and DTI metrics of WM microstructure: Potential underlying mechanisms

Glial cell activation is a common response to inflammatory processes and neuronal stress [27]. Glial cells are involved in the clearance of cell debris and axonal myelination and remyelination processes [28, 29]. Accumulation of cerebral amyloid plaques may be associated with neuronal damage [30, 31], which may induce increasing glial cell activation. Accordingly, a study using a triple transgenic mouse model of AD showed significant increases in the activation of microglia by accumulation of extracellular Aβ [32]. Moreover, a PET study in humans found significant increases in microglial activation of about 20–35% in AD patients compared to healthy controls [33]. The gliosis may restrict the diffusion of water molecules and therefore underlie the observed increases in global FA and decreases in global DR and MD with increasing amyloid at low levels of amyloid burden. At higher levels of amyloid burden, neurodegenerative effects (e.g., demyelination, axonal loss) of increasing amyloid deposition may outweigh compensating effects of

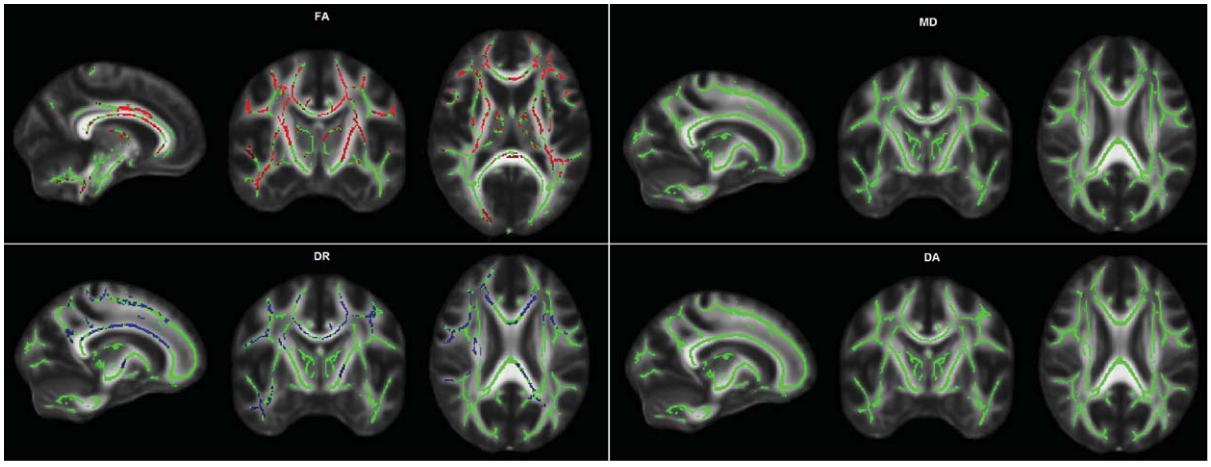

Fig. 3. Illustration of the voxel-wise quadratic polynomial regression analyses using Tract-based spatial statistic (TBSS). Diffusion-tensor imaging based metrics of white matter (WM) microstructure were set as dependent variables (fractional anisotropy, FA; mean diffusivity, MD; radial diffusivity, DR; axial diffusivity, DA). Cerebral amyloid deposition and its squared term, age as well as WM hypointensities were set as covariates. Quadratic associations between amyloid load and WM microstructure are projected onto a cerebral white matter skeleton (green). Inverted u-shaped associations are given in red. U-shaped associations are given in blue. Statistical significance was set at $p < 0.05$, corrected for multiple comparisons using threshold-free cluster enhancement.

glial cell activation (e.g., (re)myelination processes) and lead to decreases in global FA and increases in global DR and MD.

Amyloid deposition may also have a direct influence on the extent of the diffusion of water molecules, which might explain the observed divergent associations between amyloid deposition and WM microstructure at low and higher amyloid burden. At early stages of amyloid accumulation, amyloid may not yet be associated with significant neuronal atrophy. However, it may serve as a barrier and restrict diffusion. In accordance with this hypothesis, a study on AβPP transgenic mice found reduced diffusivity in the neocortex that was related to fibrillar amyloid deposits, suggesting that extracellular deposition of fibrillar amyloid restricts diffusion [34]. At higher amyloid load, increasing amyloid deposition may lead to significant neuronal death that may cause increases in diffusion.

Analyses of global and regional WM microstructure

Analyses of global WM microstructure demonstrated a strong non-linear (quadratic) association between global FA, DR, as well as MD and cerebral amyloid load. These results suggest a global effect of amyloid load on WM microstructure. In line with these results, associations between amyloid load and FA as well as DR observed in the voxel-wise TBSS regression analyses were widely distributed throughout large parts of the WM skeleton. Quadratic associations have been found in several WM tracts, including corpus callosum, fornix, corona radiata, internal capsule, and cingulum.

Studies on the relationship between cerebral amyloid load and WM microstructure in healthy older adults are rare. A recent study by Kantarci et al. demonstrated lower FA in cognitively healthy older adults with higher amyloid load (PiB SUVR >1.69) compared to subjects with lower amyloid load (PiB SUVR <1.40) in widespread WM regions (fornix, corpus callosum, occipital lobe- and parahippocampal WM). In line with our results, these findings indicate a global effect of amyloid on WM microstructure in cognitively healthy elderly. However, this finding was restricted to subjects that demonstrated coexisting gray matter neurodegeneration. Without neurodegeneration, no differences in WM microstructure between both groups have been found [35]. Another study by Racine et al. investigated a group of cognitively healthy older adults at risk for AD. In contrast to our results, the authors found higher FA and lower MD in participants with higher amyloid burden compared to participants with lower amyloid burden only in some circumscribed regions (cingulum and lateral fornix) [16]. This result indicates regionally confined effects of amyloid on WM microstructure in healthy elderly. The comparability between these studies and the present study is limited. Against the background of the observed u-shaped/inverted u-shaped associations between amyloid deposition and DTI metrics of WM microstructure in cognitively healthy elderly, it is reasonable to expect that simple group comparisons of WM microstructure between subjects with low and high amyloid burden in healthy elderly do not show any (or only small) group differences (dependent on the applied amyloid-cutoff to build the groups). As a consequence, the association between amyloid load and WM microstructure in healthy older adults may be underestimated. Further studies are necessary to confirm the observation of a global non-linear (quadratic) effect of cerebral amyloid on DTI metrics of WM microstructure in cognitively healthy elderly.

Of note, in MCI and AD patients impaired WM microstructure has mainly been found in specific WM regions, including the parahippocampal gyrus, the posterior cingulum, and the splenium of the corpus callosum [4, 5]. Accordingly, one would expect to find regional rather than global effects of cerebral amyloid load on WM microstructure. The differences in results between our study and previous studies in MCI/AD patients may be explained by different neurobiological mechanisms that underlie the observed alterations in WM microstructure with increasing amyloid load. In MCI/AD patients, impairments in WM microstructure may be a result of several neuropathological factors that occur and possibly interact (e.g., amyloid-pathology, tau-pathology) and lead to the typical pattern of WM degeneration. However, in healthy older adults incipient accumulation of Aβ in the absence of further neuropathological factors may lead to the observed global and non-linear changes in the DTI metrics of WM microstructure.

WM regions with non-coherently aligned and crossing fibers (e.g., cerebral peduncle and thalamic areas) naturally demonstrate higher isotropic diffusion [36]. In previous studies, it has been speculated that increases in WM FA with higher amyloid load may be caused by amyloid induced decreases of crossing fibers, which results in a more anisotropic diffusion [12, 14, 16]. However, our finding of rather global increases in FA and decreases in DR with increasing amyloid load at low amyloid burden casts doubts on

this hypothesis. As described in the previous section, increases in FA and decreases in DR and MD with increasing amyloid at low levels of amyloid burden may rather be explained by amyloid induced glial cell activation or by a restriction of the diffusion caused by amyloid deposits.

Present findings in the light of the preclinical AD concept

Interestingly, the vertices of the quadratic regression lines were distributed closely around the current cutoff for preclinical AD recommended for ADNI data, which is at AV45 SUVR = 1.11 [37] (vertices: global FA = 1.10, global MD = 1.14, global RD = 1.13). Impairments in global WM microstructure with increasing amyloid load may thus be characteristic of preclinical AD (and later disease stages). In line with this assumption, additionally performed linear regression analyses within a group of participants fulfilling the criteria for preclinical AD ($n = 11$) demonstrated a significant negative association between cerebral amyloid deposition and global FA ($p < 0.006$; DTI metrics of WM microstructure as dependent variables, AV45 as covariate of interest, age and WMH as covariates of no interest).

WM microstructure: Indicator of compensation and brain resilience?

Some studies demonstrated a negative association between amyloid burden and cognition in MCI/AD patients and also in cognitively healthy elderly [38–41]. In supplementary regression analyses, we investigated the association between cognitive performance and cerebral AV45 uptake, WM microstructure as well as their interaction. Interestingly, analyses demonstrated significant interaction effects between amyloid load and global WM FA, MD, DR, and DA on executive functions. These results may indicate that cognition in cognitively healthy elderly is only affected when amyloid load is increasing and WM integrity is decreasing, as observed at higher amyloid burden. At low amyloid burden, increases in FA and decreases in MD and DR with increasing amyloid load may display compensatory processes that may preserve cognitive functioning. Against the background of this compensation hypothesis one would expect a lack of an association between amyloid deposition and cognition at low amyloid burden and a negative association at higher amyloid burden. This was tested by classifying the study participants as having low and high cerebral amyloid burden (Aβ-Lo, Aβ-Hi) using the ADNI cutoff for preclinical AD (Aβ-Lo: $n = 33$, Aβ-Hi: $n = 11$). We applied partial correlation analyses between cerebral amyloid load and executive functions, controlled for age and WMH within both subgroups. In line with the compensation hypothesis, a negative association between amyloid load and executive functions has been observed in the Aβ-Hi group ($r = -0.386$) whereas no association was found in the Aβ-Lo group ($r = 0.078$). However, given the small sample size in the Aβ-Hi group the correlation analyses was underpowered (1-β = 0.36) and missed statistical significance.

Limitations

The findings of this study should be considered in the context of some limitations. First, the sample size is rather small. Although it is remarkable that we found strong effects even in this small group (that were not caused by outliers), the findings have to be replicated in a larger study group. Second, the data underlying this study were acquired on several different centers. Although strong efforts have been made to standardize data acquisition within the ADNI project, the analyses should be replicated based on a more homogeneous imaging data set. Third, histopathological studies are necessary to corroborate and help to interpret the findings of this study. Although DTI metrics are very sensitive to neurodegenerative processes, they are only indirect measures of WM microstructure. Furthermore, they are not specific to different underlying pathological processes. Finally, the study is based on a cross-sectional study design. Further studies are necessary to confirm the present findings based on longitudinal analyses.

CONCLUSIONS

The current study provides evidence for a non-linear (quadratic) relationship between cerebral amyloid deposition and DTI metrics of WM microstructure in widespread WM regions in cognitively healthy older adults. Increases in FA and decreases in MD and RD with increasing amyloid load at low levels of amyloid burden may indicate compensatory processes that may preserve cognitive functioning. At higher amyloid burden, progressive neurodegeneration may exceed compensatory mechanisms and lead to impairments in WM microstructure, which may initiate cognitive decline and facilitate the transition from asymptomatic to symptomatic stages of AD. Longi-

tudinal and histopathological studies are required to improve the understanding of mechanisms and temporal dynamics of the association between cerebral amyloid deposition and WM microstructure.

ACKNOWLEDGMENTS

Authors' disclosures available online (http://j-alz.com/manuscript-disclosures/15-0049r2).

Data collection and sharing for this project was funded by the Alzheimer's Disease Neuroimaging Initiative (ADNI) (National Institutes of Health Grant U01 AG024904) and DOD ADNI (Department of Defense award number W81XWH-12-2-0012). ADNI is funded by the National Institute on Aging, the National Institute of Biomedical Imaging and Bioengineering, and through generous contributions from the following: Alzheimer's Association; Alzheimer's Drug Discovery Foundation; BioClinica, Inc.; Biogen Idec Inc.; Bristol-Myers Squibb Company; Eisai Inc.; Elan Pharmaceuticals, Inc.; Eli Lilly and Company; F. Hoffmann-La Roche Ltd and its affiliated company Genentech, Inc.; GE Healthcare; Innogenetics, N.V.; IXICO Ltd.; Janssen Alzheimer Immunotherapy Research & Development, LLC.; Johnson & Johnson Pharmaceutical Research & Development LLC.; Medpace, Inc.; Merck & Co., Inc.; Meso Scale Diagnostics, LLC.; NeuroRx Research; Novartis Pharmaceuticals Corporation; Pfizer Inc.; Piramal Imaging; Servier; Synarc Inc.; and Takeda Pharmaceutical Company. The Canadian Institutes of Health Research is providing funds to support ADNI clinical sites in Canada. Private sector contributions are facilitated by the Foundation for the National Institutes of Health (http://www.fnih.org). The grantee organization is the Northern California Institute for Research and Education, and the study is coordinated by the Alzheimer's Disease Cooperative Study at the University of California, San Diego. ADNI data are disseminated by the Laboratory for Neuro Imaging at the University of Southern California.

REFERENCES

[1] Finder VH, Glockshuber R (2007) Amyloid-beta aggregation. *Neurodegener Dis* **4**, 13-27.

[2] Pike KE, Savage G, Villemagne VL, Ng S, Moss SA, Maruff P, Mathis CA, Klunk WE, Masters CL, Rowe CC (2007) Beta-amyloid imaging and memory in non-demented individuals: Evidence for preclinical Alzheimer's disease. *Brain* **130**, 2837-2844.

[3] Jack CR, Jr., Lowe VJ, Weigand SD, Wiste HJ, Senjem ML, Knopman DS, Shiung MM, Gunter JL, Boeve BF, Kemp BJ, Weiner M, Petersen RC, Alzheimer's Disease Neuroimaging I (2009) Serial PIB and MRI in normal, mild cognitive impairment and Alzheimer's disease: Implications for sequence of pathological events in Alzheimer's disease. *Brain* **132**, 1355-1365.

[4] Chua TC, Wen W, Slavin MJ, Sachdev PS (2008) Diffusion tensor imaging in mild cognitive impairment and Alzheimer's disease: A review. *Curr Opin Neurol* **21**, 83-92.

[5] Damoiseaux JS, Smith SM, Witter MP, Sanz-Arigita EJ, Barkhof F, Scheltens P, Stam CJ, Zarei M, Rombouts SA (2009) White matter tract integrity in aging and Alzheimer's disease. *Hum Brain Mapp* **30**, 1051-1059.

[6] Basser PJ, Mattiello J, LeBihan D (1994) MR diffusion tensor spectroscopy and imaging. *Biophys J* **66**, 259-267.

[7] Le Bihan D, Mangin JF, Poupon C, Clark CA, Pappata S, Molko N, Chabriat H (2001) Diffusion tensor imaging: Concepts and applications. *J Magn Reson Imag* **13**, 534-546.

[8] Song S-K, Sun S-W, Ramsbottom MJ, Chang C, Russell J, Cross AH (2002) Dysmyelination revealed through MRI as increased radial (but unchanged axial) diffusion of water. *Neuroimage* **17**, 1429-1436.

[9] Madden DJ, Bennett IJ, Song AW (2009) Cerebral white matter integrity and cognitive aging: Contributions from diffusion tensor imaging. *Neuropsychol Rev* **19**, 415-435.

[10] Song S-K, Kim JH, Lin S-J, Brendza RP, Holtzman DM (2004) Diffusion tensor imaging detects age-dependent white matter changes in a transgenic mouse model with amyloid deposition. *Neurobiol Dis* **15**, 640-647.

[11] Sun S-W, Song S-K, Harms MP, Lin S-J, Holtzman DM, Merchant KM, Kotyk JJ (2005) Detection of age-dependent brain injury in a mouse model of brain amyloidosis associated with Alzheimer's disease using magnetic resonance diffusion tensor imaging. *Exp Neurol* **191**, 77-85.

[12] Zerbi V, Kleinnijenhuis M, Fang X, Jansen D, Veltien A, Van Asten J, Timmer N, Dederen PJ, Kiliaan AJ, Heerschap A (2013) Gray and white matter degeneration revealed by diffusion in an Alzheimer mouse model. *Neurobiol Aging* **34**, 1440-1450.

[13] Qin Y-Y, Li M-W, Zhang S, Zhang Y, Zhao L-Y, Lei H, Oishi K, Zhu W-Z (2013) *In vivo* quantitative whole-brain diffusion tensor imaging analysis of APP/PS1 transgenic mice using voxel-based and atlas-based methods. *Neuroradiology* **55**, 1027-1038.

[14] Shu X, Qin Y-Y, Zhang S, Jiang J-J, Zhang Y, Zhao L-Y, Shan D, Zhu W-Z (2013) Voxel-based diffusion tensor imaging of an APP/PS1 mouse model of Alzheimer's disease. *Mol Neurobiol* **48**, 78-83.

[15] Chao LL, DeCarli C, Kriger S, Truran D, Zhang Y, Laxamana J, Villeneuve S, Jagust WJ, Sanossian N, Mack WJ (2013) Associations between white matter hyperintensities and β amyloid on integrity of projection, association, and limbic fiber tracts measured with diffusion tensor MRI. *PLoS One* **8**, e65175.

[16] Racine AM, Adluru N, Alexander AL, Christian BT, Okonkwo OC, Oh J, Cleary CA, Birdsill A, Hillmer AT, Murali D (2014) Associations between white matter microstructure and amyloid burden in preclinical Alzheimer's disease: A multimodal imaging investigation. *Neuroimage Clin* **4**, 604-614.

[17] Ryan NS, Keihaninejad S, Shakespeare TJ, Lehmann M, Crutch SJ, Malone IB, Thornton JS, Mancini L, Hyare H, Yousry T (2013) Magnetic resonance imaging evidence for presymptomatic change in thalamus and caudate in familial Alzheimer's disease. *Brain* **136**, 1399-1414.

[18] Grubbs FE (1950) Sample criteria for testing outlying observations. *Ann Math Stat* 27-58.
[19] Fazekas F, Chawluk JB, Alavi A, Hurtig H, Zimmerman R (1987) MR signal abnormalities at 1.5 T in Alzheimer's dementia and normal aging. *Am J Roentgenol* **149**, 351-356.
[20] Wolf D, Fischer FU, Fesenbeckh J, Yakushev I, Lelieveld IM, Scheurich A, Schermuly I, Zschutschke L, Fellgiebel A (2014) Structural integrity of the corpus callosum predicts long-term transfer of fluid intelligence-related training gains in normal aging. *Hum Brain Mapp* **35**, 309-318.
[21] Smith SM (2002) Fast robust automated brain extraction. *Hum Brain Mapp* **17**, 143-155.
[22] Basser PJ, Mattiello J, LeBihan D (1994) Estimation of the effective self-diffusion tensor from the NMR spin echo. *J Magn Reson B* **103**, 247-254.
[23] Smith SM, Jenkinson M, Johansen-Berg H, Rueckert D, Nichols TE, Mackay CE, Watkins KE, Ciccarelli O, Cader MZ, Matthews PM (2006) Tract-based spatial statistics: Voxelwise analysis of multi-subject diffusion data. *Neuroimage* **31**, 1487-1505.
[24] Rueckert D, Sonoda LI, Hayes C, Hill DL, Leach MO, Hawkes DJ (1999) Nonrigid registration using free-form deformations: Application to breast MR images. *IEEE Trans Med Imaging* **18**, 712-721.
[25] Gibbons LE, Carle AC, Mackin RS, Harvey D, Mukherjee S, Insel P, Curtis SM, Mungas D, Crane PK, Initiative AsDN (2012) A composite score for executive functioning, validated in Alzheimer's Disease Neuroimaging Initiative (ADNI) participants with baseline mild cognitive impairment. *Brain Imaging Behav* **6**, 517-527.
[26] Crane PK, Carle A, Gibbons LE, Insel P, Mackin RS, Gross A, Jones RN, Mukherjee S, Curtis SM, Harvey D (2012) Development and assessment of a composite score for memory in the Alzheimer's Disease Neuroimaging Initiative (ADNI). *Brain Imaging Behav* **6**, 502-516.
[27] Jauregui-Huerta F, Ruvalcaba-Delgadillo Y, Gonzalez-Castaneda R, Garcia-Estrada J, Gonzalez-Perez O, Luquin S (2010) Responses of glial cells to stress and glucocorticoids. *Current Immunol Rev* **6**, 195-204.
[28] Olah M, Amor S, Brouwer N, Vinet J, Eggen B, Biber K, Boddeke HW (2012) Identification of a microglia phenotype supportive of remyelination. *Glia* **60**, 306-321.
[29] Doring A, Yong V (2010) The good, the bad and the ugly. Macrophages/microglia with a focus on myelin repair. *Front Biosci (Schol Ed)* **3**, 846-856.
[30] Hardy J, Selkoe DJ (2002) The amyloid hypothesis of Alzheimer's disease: Progress and problems on the road to therapeutics. *Science* **297**, 353-356.
[31] Tanzi R, Moir R, Wagner S (2004) Clearance of Alzheimer's Aβ peptide: The many roads to perdition. *Neuron* **43**, 605-608.
[32] Rodriguez J, Witton J, Olabarria M, Noristani H, Verkhratsky A (2010) Increase in the density of resting microglia precedes neuritic plaque formation and microglial activation in a transgenic model of Alzheimer's disease. *Cell Death Dis* **1**, e1.
[33] Edison P, Archer HA, Gerhard A, Hinz R, Pavese N, Turkheimer FE, Hammers A, Tai YF, Fox N, Kennedy A (2008) Microglia, amyloid, and cognition in Alzheimer's disease: An [11C](R) PK11195-PET and [11C] PIB-PET study. *Neurobiol Dis* **32**, 412-419.
[34] Mueggler T, Meyer-Luehmann M, Rausch M, Staufenbiel M, Jucker M, Rudin M (2004) Restricted diffusion in the brain of transgenic mice with cerebral amyloidosis. *Eur J Neurosci* **20**, 811-817.
[35] Kantarci K, Schwarz CG, Reid RI, Przybelski SA, Lesnick TG, Zuk SM, Senjem ML, Gunter JL, Lowe V, Machulda MM (2014) White matter integrity determined with diffusion tensor imaging in older adults without dementia: Influence of amyloid load and neurodegeneration. *JAMA Neurol* **71**, 1547-1554.
[36] Alexander AL, Hurley SA, Samsonov AA, Adluru N, Hosseinbor AP, Mossahebi P, Tromp DP, Zakszewski E, Field AS (2011) Characterization of cerebral white matter properties using quantitative magnetic resonance imaging stains. *Brain Connect* **1**, 423-446.
[37] Landau S, Jagust W (2011) Florbetapir processing methods. http://adni.bitbucket.org/docs/UCBERKELEYAV45/ADNI_AV45_Methods_JagustLab_04.29.14.pdf. Revised April 29, 2014.
[38] Hedden T, Oh H, Younger AP, Patel TA (2013) Meta-analysis of amyloid-cognition relations in cognitively normal older adults. *Neurology* **80**, 1341-1348.
[39] Braskie MN, Thompson PM (2013) Understanding cognitive deficits in Alzheimer's disease based on neuroimaging findings. *Trends Cogn Sci* **17**, 510-516.
[40] Forsberg A, Engler H, Almkvist O, Blomquist G, Hagman G, Wall A, Ringheim A, Långström B, Nordberg A (2008) PET imaging of amyloid deposition in patients with mild cognitive impairment. *Neurobiol Aging* **29**, 1456-1465.
[41] Edison P, Archer H, Hinz R, Hammers A, Pavese N, Tai Y, Hotton G, Cutler D, Fox N, Kennedy A (2007) Amyloid, hypometabolism, and cognition in Alzheimer disease An [11C] PIB and [18F] FDG PET study. *Neurology* **68**, 501-508.